Int J Earth Sci (Geol Rundsch) (2017) 106:1487–1504
DOI 10.1007/s00531-016-1362-8

ORIGINAL PAPER

Polychronous (Early Cretaceous to Palaeogene) emplacement of the Mundwara alkaline complex, Rajasthan, India: $^{40}Ar/^{39}Ar$ geochronology, petrochemistry and geodynamics

Kanchan Pande[1] · Ciro Cucciniello[2] · Hetu Sheth[1] · Anjali Vijayan[1] · Kamal Kant Sharma[3] · Ritesh Purohit[3] · K. C. Jagadeesan[4] · Sapna Shinde[1]

Received: 8 March 2016 / Accepted: 20 June 2016 / Published online: 18 July 2016

Abstract The Mundwara alkaline plutonic complex (Rajasthan, north-western India) is considered a part of the Late Cretaceous–Palaeogene Deccan Traps flood basalt province, based on geochronological data (mainly $^{40}Ar/^{39}Ar$, on whole rocks, biotite and hornblende). We have studied the petrology and mineral chemistry of some Mundwara mafic rocks containing mica and amphibole. Geothermobarometry indicates emplacement of the complex at middle to upper crustal levels. We have obtained new $^{40}Ar/^{39}Ar$ ages of 80–84 Ma on biotite separates from mafic rocks and 102–110 Ma on whole-rock nepheline syenites. There is no evidence for excess ^{40}Ar. The combined results show that some of the constituent intrusions of the Mundwara complex are of Deccan age, but others are older and unrelated to the Deccan Traps. The Mundwara alkaline complex is thus polychronous and similar to many alkaline complexes around the world that show recurrent magmatism, sometimes over hundreds of millions of years. The primary biotite and amphibole in Mundwara mafic rocks indicate hydrous parental magmas, derived from hydrated mantle peridotite at relatively low temperatures, thus ruling out a mantle plume. This hydration and metasomatism of the Rajasthan lithospheric mantle may have occurred during Jurassic subduction under Gondwanaland, or Precambrian subduction events. Low-degree decompression melting of this old, enriched lithospheric mantle, due to periodic diffuse lithospheric extension, gradually built the Mundwara complex from the Early Cretaceous to Palaeogene time.

Keywords India · Rajasthan · Mundwara alkaline complex · Biotite · Amphibole · $^{40}Ar/^{39}Ar$ dating

Introduction

The Mundwara plutonic complex in Rajasthan, north-western India (Fig. 1), is a superb field museum of alkaline igneous rocks including gabbros, essexites, pyroxenites, ijolites, basanites, lamprophyres and nepheline syenites, as well as carbonatites (Coulson 1933; Bose and Das Gupta 1973; Viswanathan 1977; Subrahmanyam and Rao 1977; Chakraborti and Bose 1978; Chakraborti 1979; Subrahmanyam and Leelanandam 1989, 1991; Srivastava 1989). The Mundwara complex is emplaced in the Erinpura Granite, a polychronous assemblage of various granitoid plutons ~1100–850 Ma in age (Just et al. 2011; Dharma Rao et al. 2013). Granites and rhyolites of the ~750 Ma Malani igneous province (Eby and Kochhar 1990; Tucker et al. 2001; Bhushan and Chandrasekaran 2002) cover large parts of the region. No other indications to the age of the Mundwara complex are available from outcrop geology. Subrahmanyam et al. (1972) reported an apatite fission track date of 56 ± 8 Ma on a theralite. Basu

Electronic supplementary material The online version of this article (doi:10.1007/s00531-016-1362-8) contains supplementary material, which is available to authorized users.

✉ Hetu Sheth
hcsheth@iitb.ac.in

[1] Department of Earth Sciences, Indian Institute of Technology Bombay, Powai, Mumbai 400076, India

[2] Dipartimento di Scienze della Terra, dell'Ambiente e delle Risorse (DiSTAR), Università di Napoli Federico II, via Mezzocannone 8, 80134 Naples, Italy

[3] Department of Geology, Government Postgraduate College, Sirohi, Rajasthan 307001, India

[4] Isotope Production and Application Division, Bhabha Atomic Research Centre (BARC), Mumbai 400085, India

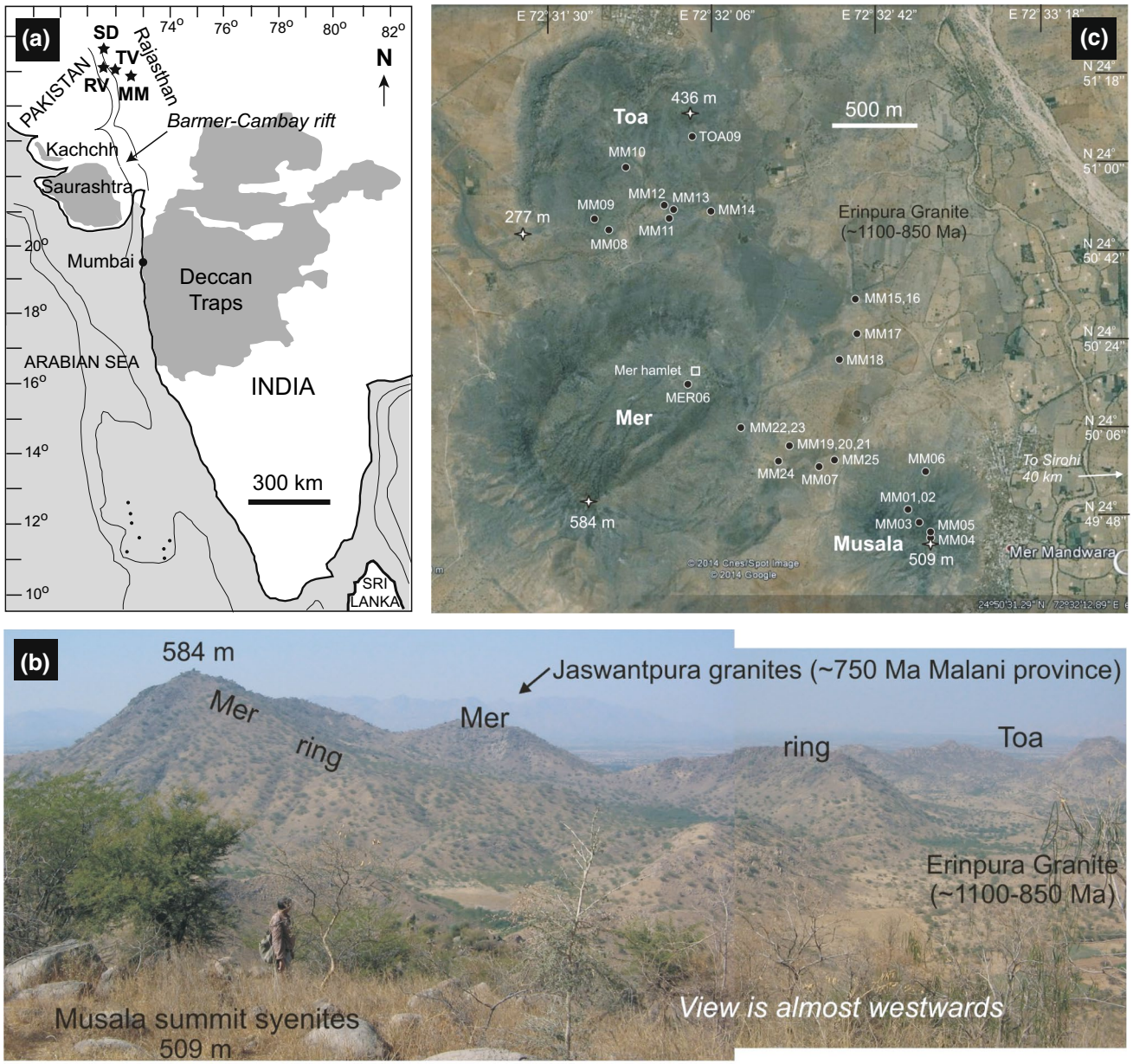

Fig. 1 **a** Map of India and the Deccan Traps (*shaded*) with volcano-plutonic complexes in Rajasthan marked. *SD* is Sarnu-Dandali complex, *TV* the Tavidar volcanics and *RV* the Raageshwari volcanics, all of which are related to Deccan flood volcanism and lie within or adjacent to the Barmer-Cambay rift. *MM* is the Mer Mundwara (simply, Mundwara) complex, outside the Barmer-Cambay rift. Based on Bladon et al. (2015) and Vijayan et al. (in press). **b** Panoramic view of the Mundwara complex, from the summit of the Musala pluton. **c** Google Earth image of the Mundwara complex with the sample locations marked. The locations of samples MER06 and TOA09 are approximate

et al. (1993) and Rathore et al. (1996) provided $^{40}Ar/^{39}Ar$ ages of ~68.5–64 Ma on mineral separates (primary biotite and amphibole) and whole-rock samples from the complex. Based on these age data, the Mundwara complex is considered to be a distant outlier of the ~65 Ma (Late Cretaceous to Palaeogene) Deccan Traps flood basalt province (Fig. 1a) (e.g. Subrahmanyam et al. 1972; Basu et al. 1993; Rathore et al. 1996; Bhushan and Chandrasekaran 2002).

Though many workers have studied the petrology of Mundwara rocks (references above), the petrogenetic significance of the primary hydrous minerals (biotite and amphibole) in the Mundwara mafic rocks has been little discussed. We have carried out a petrographic and mineral

chemical study of select mafic rocks of the complex and derived thermobarometric results. More importantly, we have obtained new $^{40}Ar/^{39}Ar$ ages of 80–84 Ma on primary biotites in these mafic rocks and of 102–110 Ma on nepheline syenite whole rocks. The $^{40}Ar/^{39}Ar$ ages, significantly higher than those provided by previous workers, are robust and not affected by excess argon. We interpret the combined $^{40}Ar/^{39}Ar$ age data as indicating a polychronous emplacement history of the Mundwara complex, from Early Cretaceous time to Late Cretaceous and Palaeogene time (Deccan volcanism). We discuss the important geodynamic implications of the primary biotite and amphibole and the significantly pre-Deccan components in the Mundwara complex. Our results considerably improve the current understanding of the Mesozoic magmatic history and crustal evolution in north-western India.

Geology and samples

The Mundwara complex, 40 km WSW of Sirohi town in south-western Rajasthan, covers an area of about 15 km^2. It is composed of three individual plutons. The largest, Mer, forms a ring intrusion rising ~300 m above surrounding flat plains of the basement granite (Fig. 1b, c). The Toa pluton forms a partial ring, whereas the Musala pluton (Fig. 1b, c) may have been a laccolithic plug. Each of these plutons is made up of a large number of constituent intrusions. Mer shows a range of rock types like gabbro, nepheline syenite, theralite and melteigite, Toa dominantly contains cumulate gabbros and pyroxenites with minor nepheline syenite, whereas Musala shows essexite below and nepheline syenite above. The chilled margin of the complex is of basanite composition (Subrahmanyam and Leelanandam 1989), and the three plutons are cut by hundreds of dykes and veins of basanites, nepheline syenites, lamprophyres, tephriphonolites and carbonatites (Viswanathan 1977; Subrahmanyam and Leelanandam 1989). We collected many of these rocks in December 2012 (samples MM01–MM24, Fig. 1c), and our sample set also includes a gabbroic sample (MER06) and a nepheline syenite (TOA09) collected during a previous field visit in December 2004.

Rock nomenclature and petrography

The Mundwara mafic rocks have been named based on their modal compositions, which were obtained using the Leica QwinPlus software image analysis (counting 1500 points in each thin section). In the QAPF diagram of Streckeisen (1974; Fig. 2), these rocks cover a range from gabbro to monzodiorite, theralite and essexite. Cumulate textures are common. All grain sizes mentioned in the text refer to measurements of the long dimension.

Sample MM03 from the Musala pluton (Fig. 3a, b) is an essexite. It shows an inequigranular hypidiomorphic

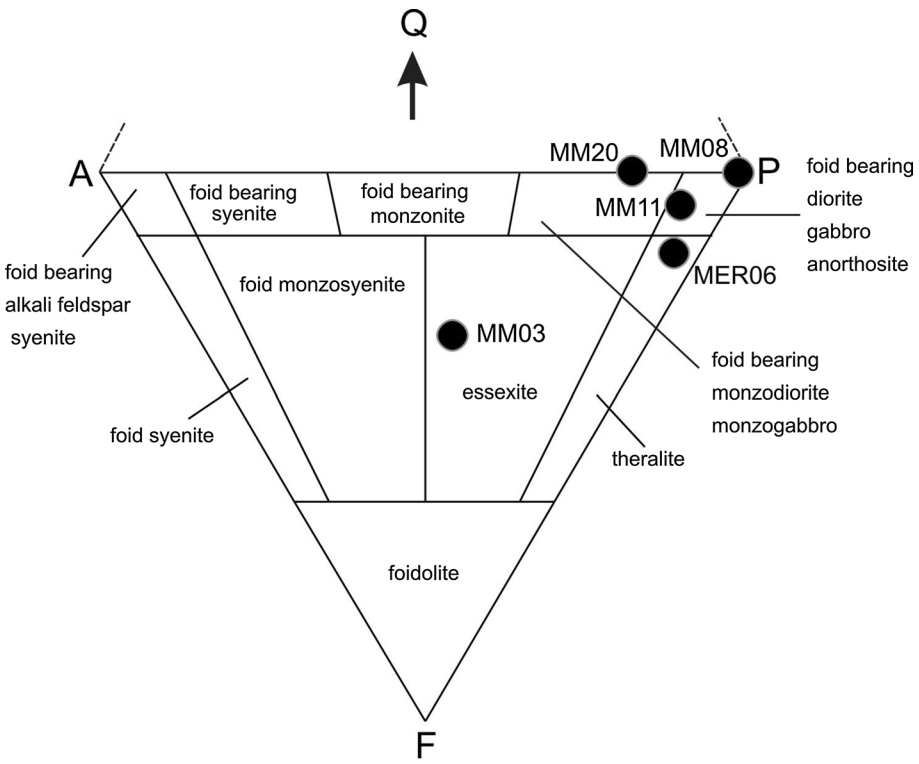

Fig. 2 Classification of the Mundwara rocks according to their modal mineral contents on the QAPF plot of Streckeisen (1974). *Q* is quartz, *A* is alkali feldspar, *P* is plagioclase, and *F* is feldspathoid

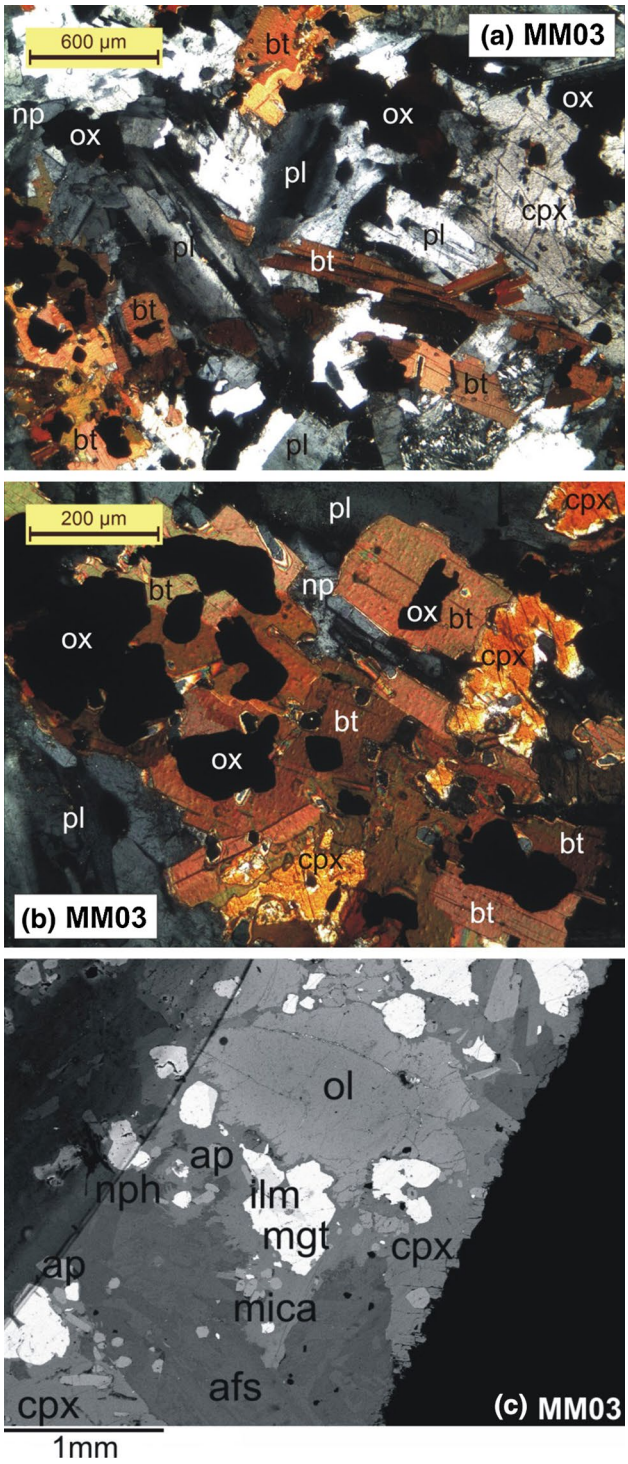

Fig. 3 Petrography of Mundwara essexite MM03. **a**, **b** Photomicrographs, taken between crossed polars. Mineral names are abbreviated as *pl* (plagioclase), *cpx* (clinopyroxene), *np* (nepheline), *bt* (biotite), ox (Fe–Ti oxide). **c** Backscattered electron (BSE) image of essexite MM03: hypidiomorphic texture showing olivine, clinopyroxene, Fe–Ti oxides, mica, feldspars, nepheline and apatite. *Abbreviations*: *ol* olivine, *pl* plagioclase, *cpx* clinopyroxene, *mgt* magnetite, *ilm* ilmenite, *afs* alkali feldspar, *nph* nepheline, *amp* amphibole, *tit* titanite, *ap* apatite, *anl* analcime

texture. The essential minerals are euhedral to subhedral clinopyroxene (32 %), interstitial alkali feldspars (15 %), plagioclase (18 %) and nepheline (10 %). Accessory minerals include Fe–Ti oxides (8 %), mica (8 %), olivine (5 %) and apatite (3 %). Olivine grains are normally zoned, often mantled by mica or clinopyroxene (Fig. 3c).

Sample MM08 from the Toa pluton (Fig. 4a, b) is an olivine gabbro. It contains olivine (20 %), plagioclase (48 %) and clinopyroxene (27 %). Common accessory phases are mica (<3 %), Fe–Ti oxides (<5 %) and apatite (~1 %). Olivine crystals are commonly subhedral or anhedral and ~0.2 to ~2.5 mm in size. They are unzoned and generally altered to iddingsite along fractures. Small olivine crystals are enclosed in large grains of clinopyroxene (rarely, plagioclase) forming poikilitic texture (Fig. 4b). Plagioclase occurs generally as euhedral to subhedral lath-shaped cumulus crystals with lengths varying from ~0.5 to ~2 mm. Clinopyroxenes occur as subhedral to anhedral crystals of the same size and generally enclose small olivine and plagioclase grains. Fe–Ti oxides (magnetite and ilmenite) occur as 0.1–1.0 mm irregular interstitial grains. Mica is an interstitial phase, often mantling Fe–Ti oxides. Apatite (~50 µm) occurs as inclusions in plagioclase crystals.

Sample MM11, also from the Toa pluton, is a foid-bearing diorite (Fig. 4c, d). The main minerals are plagioclase (28 %) and clinopyroxene (38 %), followed by mica (8 %), amphibole (9 %), alkali feldspars (5 %), Fe–Ti oxides (10 %), titanite (1 %) and apatite (1 %). It shows a poikilitic texture (Fig. 4c, d). Large plagioclase and amphibole crystals enclose small grains of clinopyroxene, mica and Fe–Ti oxides. Textural relationships show that the clinopyroxene and plagioclase predate the amphibole and mica. Nepheline crystals have been replaced by analcime (Fig. 4d).

The sample MM20 from the outer eastern slopes of the Mer pluton is a monzodiorite (Fig. 4e, f). It shows a poikilitic texture and consists of clinopyroxene (33 %), plagioclase (28 %), mica (13 %), Fe–Ti oxides (9 %), alkali feldspars (10 %), amphibole (4 %) titanite (2 %) and apatite (1 %). Plagioclase and alkali feldspars occur generally as euhedral or subhedral crystals up to 2.5 mm in size. The crystals are randomly oriented and commonly enclose crystals of clinopyroxene, mica, amphibole, Fe–Ti oxides, titanite and apatite. The alkali feldspar is often perthitic. Clinopyroxene-crystals are typically euhedral to subhedral, 0.2–1 mm long, and have a prismatic to tabular habit. Mica occurs as euhedral to subhedral platy crystals with lengths up to 1.5 mm. It is generally enclosed in large plagioclase or alkali feldspar grains. The amphibole crystals (more or less corroded) range in size from 0.5 to 1 mm and generally enclose small clinopyroxene, Fe–Ti oxides and mica grains (Fig. 4e, f). Fe–Ti oxides occur as 0.1–0.5 mm euhedral to subhedral grains in plagioclase, alkali feldspars and amphibole crystals.

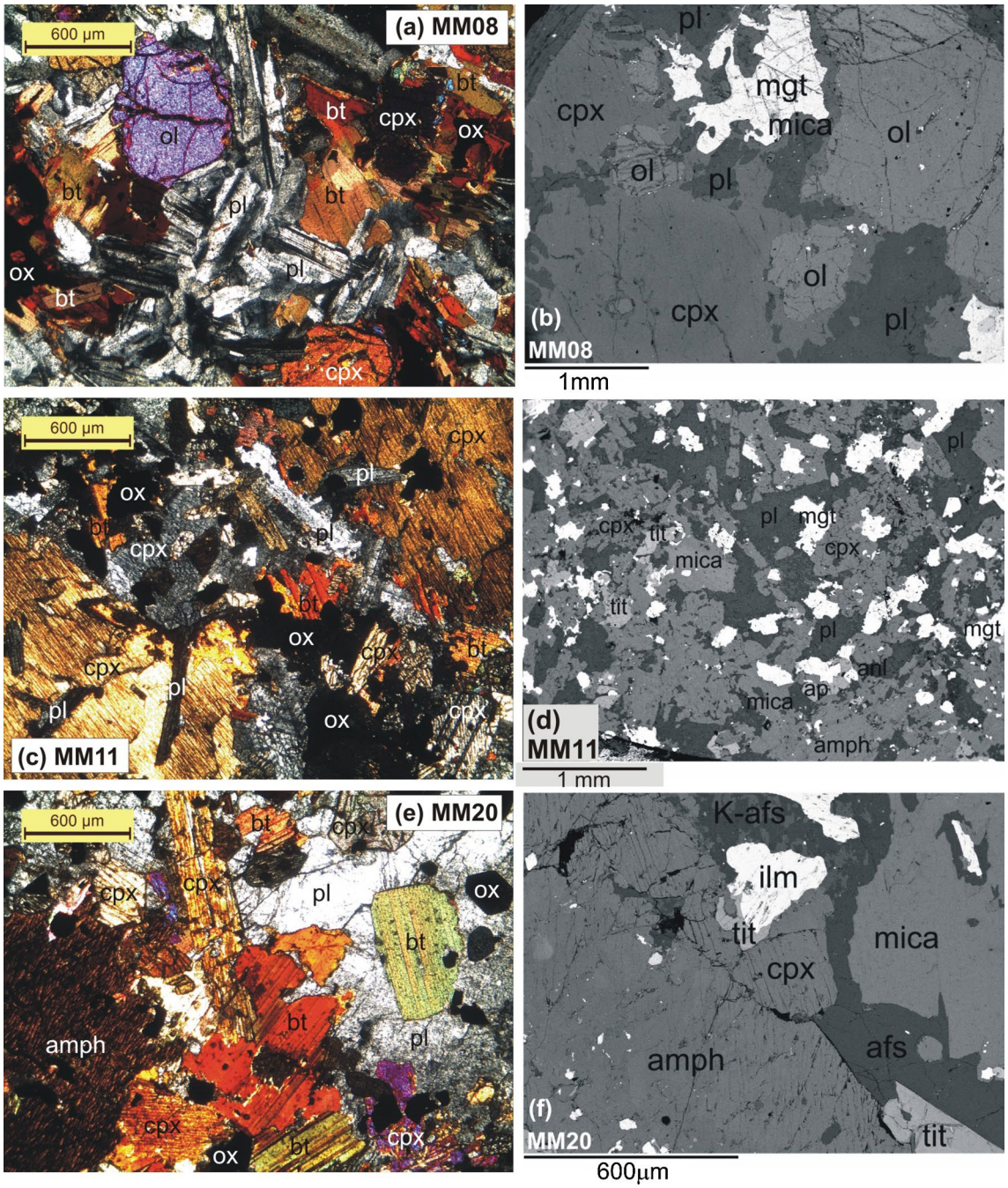

Fig. 4 Petrography of Mundwara mafic rocks. Photomicrographs and BSE images for Mundwara olivine gabbro MM08 (**a**, **b**), foid-bearing diorite MM11 (**c**, **d**), and monzodiorite MM20 (**e**, **f**). The BSE image of olivine gabbro MM08 (**b**) shows poikilitic texture. Small olivine grains are enclosed in large clinopyroxene. The BSE image of foid-bearing diorite MM11 (**d**) shows clinopyroxene and Fe–Ti oxides enclosed in large plagioclase crystals. The BSE image of monzodiorite MM20 (**f**) shows large amphibole crystal enclosing small Fe–Ti oxides grains. Alkali feldspars occupy the angular interstices between amphibole, mica and clinopyroxene grains

The sample MER06, collected near Mer hamlet inside the Mer ring (Fig. 1c), is a theralite (Fig. 5a–c). It is a medium-grained rock composed of plagioclase (38 %), clinopyroxene (26 %), mica (11 %), olivine (8 %), Fe–Ti oxides (9 %), nepheline (5 %) and apatite (3 %). Olivine grains have sizes of 0.1–1.5 mm and commonly are enclosed in clinopyroxene and mica crystals. They are normally zoned with slight core to rim variations. Plagioclase occurs as subhedral laths ranging from 0.2 to 2 mm in width. Clinopyroxene occurs as euhedral to subhedral

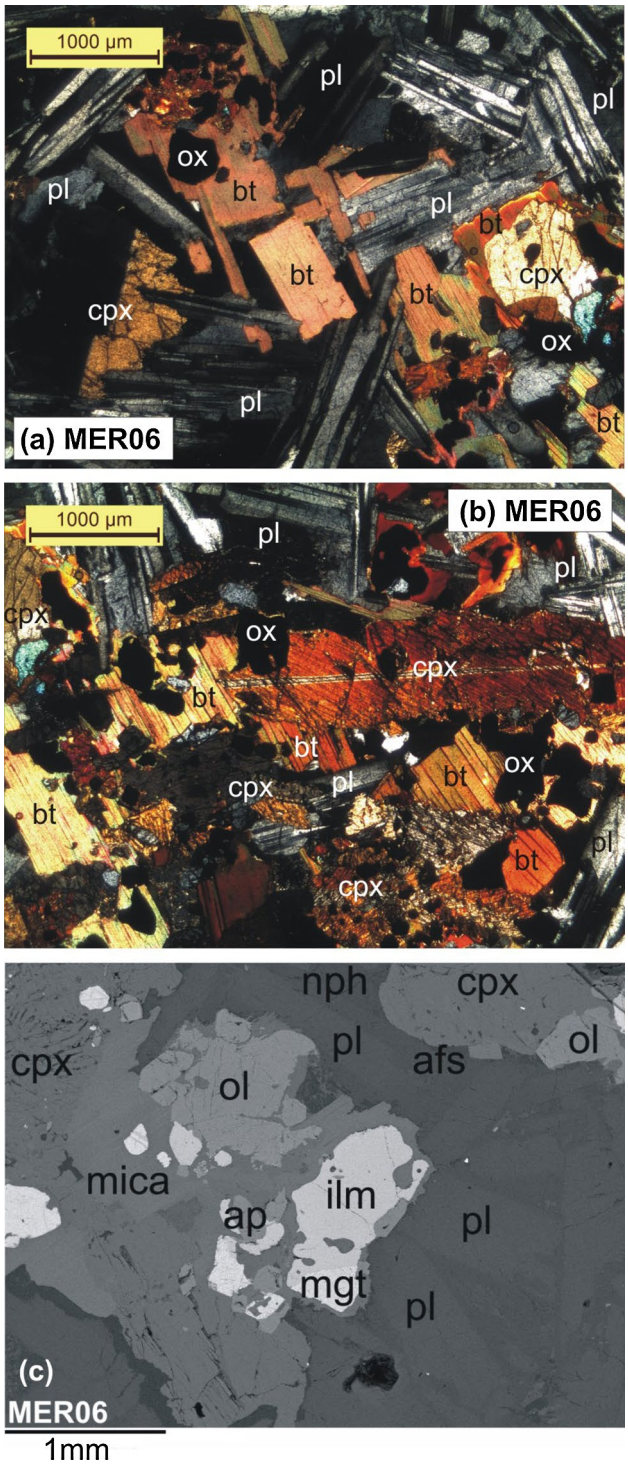

Fig. 5 Petrography of Mundwara theralite MER06. **a**, **b** Photomicrographs taken between crossed polars. **c** BSE image showing plagioclase, clinopyroxene, mica, olivine, Fe–Ti oxides and minor amounts of alkali feldspars, nepheline and apatite

crystals 1–3.5 mm in size. It commonly contains small grains of olivine, Fe–Ti oxides, apatite and rarely mica. Mica occurs either as subhedral medium crystals or as interstitial and poikilitic grains. Nepheline occurs as anhedral interstitial grains (Fig. 5a–c).

Dyke sample MM24 is broadly a tephriphonolite, with phenocrysts of biotite and amphibole and a fine-grained groundmass with alkali feldspar, iron oxides and some clinopyroxene (Fig. 6a). Petrography of the Mundwara nepheline syenites has been described in detail by several workers including Bose and Das Gupta (1973), Chakraborti (1979) and Subrahmanyam and Leelanandam (1989). The nepheline syenites are dominated by alkali feldspars, with subordinate amounts of nepheline, clinopyroxene and biotite, as well as accessory phases like iron oxides, sphene, apatite, sodalite, calcite and zircon. The nepheline syenite samples MM04 (from Musala hill summit), MM21 (a dyke on the outer slopes of Mer) and TOA09 (an intrusion in the Toa pluton) are shown in Fig. 6b–d. The first two are fine to medium grained and relatively fresh, whereas TOA09 has a highly weathered appearance.

Whole-rock geochemistry

The mafic rocks and a nepheline syenite (MM04) were analysed by inductively coupled plasma atomic emission spectrometry (ICPAES) at the Sophisticated Analytical Instrumentation Facility (SAIF), IIT Bombay (instrument: SPECTRO ARCOS), for all major oxides and a few trace elements (Table 1). The analytical procedures followed Vijayan et al. (in press). Several USGS mafic rock standards (DNC-1, BIR-1, BCR-2 and AGV-2) were dissolved along with the samples and used for calibrating the instrument, whereas the standard W-2a was analysed as an unknown to estimate the analytical accuracy. Loss on ignition (LOI) values were determined by heating the rock powders at 1000 °C in platinum crucibles, after overnight drying in an oven at 110 °C to drive away adsorbed moisture (H_2O^-).

The major oxide, LOI and trace element values for the Mundwara mafic rocks are presented in Table 1, along with the reference and measured values on standard W-2a. The high analytical accuracy is indicated by the very close reference and measured values for W-2a. All analyses have major oxide and LOI totals that are nearly 100 wt%. CIPW norms and Mg numbers (Mg#) computed for all samples using the SINCLAS program of Verma et al. (2002) are also presented in Table 1. All rocks are nepheline normative.

Mineral chemistry and thermobarometry

Analytical techniques

Mineral compositions in the mafic rocks were obtained at the University of Naples, using an Oxford Instruments

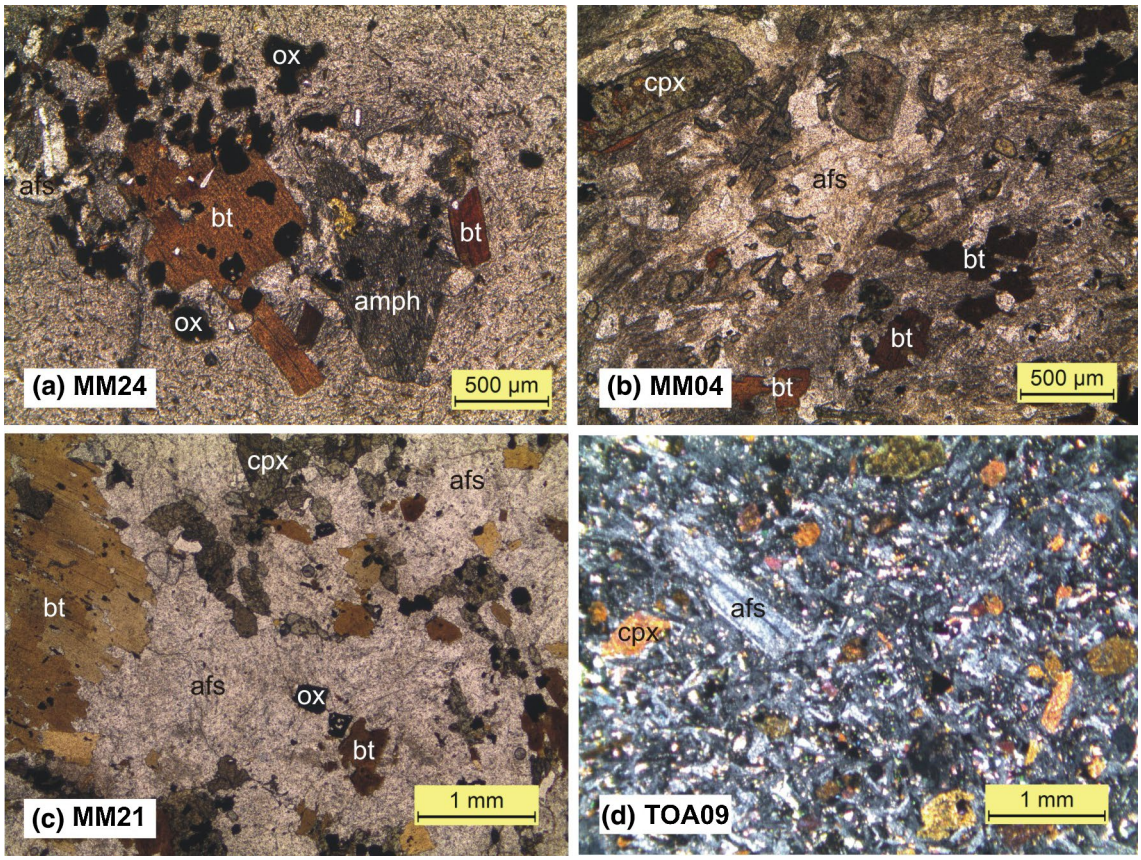

Fig. 6 Petrography of the Mundwara tephriphonolite MM24 (**a**) and nepheline syenites MM04 (**b**), MM21 (**c**) and TOA09 (**d**). *Abbreviations*: *afs* alkali feldspar, *amph* amphibole, *bt* biotite, *ox* iron oxides, *cpx* clinopyroxene. All photomicrographs are over the polarizer

Microanalysis Unit equipped with an INCA X-act detector and a JEOL JSM-5310 microscope in energy-dispersive spectrometry (EDS). The standard operating conditions included a primary beam voltage of 15 kV, filament current of 50–100 µA and variable spot size from 30,000 to 200,000× magnification, 20 mm WD. Measurements were taken with an INCA X-stream pulse processor and with Energy software. Energy uses the XPP matrix correction scheme, developed by Pouchou and Pichoir (1988), and the pulse pile-up correction. The quant optimization is carried out using cobalt (FWHM—full width at half maximum peak height—of the strobed zero = 60–65 eV). The following standards were used for calibration: diopside (Ca), San Carlos olivine (Mg), anorthoclase (Al, Si), albite (Na), rutile (Ti), fayalite (Fe), Cr_2O_3 (Cr), rhodonite (Mn), orthoclase (K), apatite (P), fluorite (F), barite (Ba), strontianite (Sr), zircon (Zr, Hf), synthetic Smithsonian orthophosphates (REE, Y, Sc), pure vanadium, niobium and tantalum (V, Nb, Ta), Corning glass (Th and U), sphalerite (S, Zn), galena (Pb), sodium chloride (Cl) and pollucite (Cs). The Ka, La, Lb or Ma lines were used for calibration, according to the element. Backscattered electron (BSE) images were obtained with the same instrument. Representative microprobe analyses of the various mineral phases are reported in Supplementary Tables S1-1–S1-11.

Mineral compositions

Olivine

Olivine from the olivine gabbro MM08 shows a restricted range of composition from Fo_{62} to Fo_{65} (where Fo = Mg/(Mg + Fe) × 100; Fig. 7a). NiO is variable and ranges from below detection limit to 0.36 wt%. CaO does not exceed 0.28 wt%. Olivine from theralite MER06 has Fo values from 50 to 58 mol%. NiO and CaO contents are low. Olivine of the essexite MM03 has Fo values between 51 and 65 mol% and contains <0.24 wt% NiO.

Clinopyroxene

Clinopyroxene is an essential phase in all studied rocks. According to the nomenclature scheme of Morimoto et al. (1988), it is diopside ($Ca_{49–46}Mg_{33–43}Fe_{18–11}$; Fig. 7b). The Mg# [where Mg# = atomic Mg*100/(Mg + Fe + Mn)] values of clinopyroxenes are 73–75, 72–80, 69–81, 65–76

Table 1 Whole-rock geochemical data for Mundwara plutonic rocks

Lat. (N)	24°49.732′	24°50.759′	24°50.818′	24°50.068′	24°50.013′	–	24°49.732′		
Long. (E)	72°32.868′	72°31.726′	72°31.965′	72°32.381′	72°32.334′	–	72°32.868′		
Sample	MM03	MM08	MM11	MM20	MM24	MER06	MM04	W-2a	W-2a
Rock type	Essexite	Ol. gabbro	Foid diorite	Monzodior.	Tephriph.	Theralite	Ne.syen.	Ref.	Meas.
SiO_2	42.89	45.53	42.42	46.67	49.17	41.02	54.11	52.68	52.71
TiO_2	3.64	2.07	4.88	4.04	2.06	5.46	1.73	1.06	1.09
Al_2O_3	13.63	15.02	10.67	10.92	17.48	13.38	17.76	15.45	15.08
Fe_2O_{3T}	15.44	12.96	17.08	14.97	9.25	14.84	7.08	10.83	11.74
MnO	0.30	0.18	0.23	0.21	0.26	0.24	0.18	0.167	0.12
MgO	5.35	9.97	7.81	6.63	2.21	6.52	2.12	6.37	6.69
CaO	8.90	11.37	13.47	10.05	4.01	11.11	4.09	10.86	10.84
Na_2O	4.86	2.47	2.40	3.24	7.90	3.32	8.05	2.20	2.23
K_2O	2.32	0.55	1.33	2.10	5.07	1.40	4.54	0.626	0.49
P_2O_5	1.81	0.22	0.47	0.67	1.06	1.33	0.49	0.14	0.12
LOI	−0.06	−0.15	0.57	0.23	2.66	0.71	0.60		
Total	99.08	100.19	101.34	99.73	101.14	99.33	100.74	100.38	101.11
Mg#	46.6	64.3	51.7	52.7	39.2	50.7	44.7		
Or	14.00	3.27	7.91	12.62	30.64	8.50	26.93		
Ab	14.47	16.02	3.13	20.62	12.68	11.39	27.14		
An	8.70	28.49	14.51	9.21	–	17.94	–		
Ne	14.91	2.73	9.38	3.93	27.30	9.46	21.22		
Di	20.04	21.83	40.68	30.22	11.09	24.25	14.17		
Ol	11.67	20.29	10.14	9.32	5.82	11.27	2.47		
Mt	4.86	2.89	3.80	4.69	1.30	3.37	1.82		
Il	7.06	3.96	9.33	7.80	4.00	10.65	3.30		
Ap	4.28	0.51	1.10	1.58	2.51	3.16	1.14		
Ac			–		4.66		1.81		
Sc	15.9	28.4	42.4	30.2	4.55	26.7	6.60	36	36.9
Co	49.3	54.0	80.8	50.8	30.8	64.1	26.9	43	35.7
Ni	25.7	95.6	73.7	55.0	14.5	16.7	22.5	70	71.4
Sr	1864	671	668	594	1425	1107	1305	190	196
Zr	230	117	314	379	801	150	888	100	91.8
Ba	1014	252	481	509	1017	631	1023	170	174

Major oxides are in wt% and the trace elements in parts per million (ppm). Fe_2O_{3T} is total iron expressed as Fe_2O_3. Abbreviated mineral names in italics are CIPW normative minerals (in wt%) as computed by the SINCLAS program of Verma et al. (2002), based on LOI-free recalculated data and the Middlemost (1989) scheme of division of total iron into Fe^{2+} and Fe^{3+} categories. Reference and measured values on the USGS standard W-2a (Wilson, http://crustal.usgs.gov/geochemical_reference_standards/powdered_RM.html) provides an idea about analytical accuracy

and 72–75 in the essexite MM03, olivine gabbro MM08, foid-bearing diorite MM11, monzodiorite MM20 and theralite MER06, respectively. TiO_2 and Al_2O_3 contents range from 0.12 to 3.67 and from 0.72 to 7.03 wt%, respectively. Cr_2O_3 ranges from below detection limit to 0.25 wt%.

Feldspars

Euhedral to subhedral feldspars of variable size are present in all rock types, and almost pure albite laths occur in some late-stage mineral associations. In the essexite MM03, plagioclase is an andesine (An_{38}). Alkali feldspars range from anorthoclase ($An_7Ab_{62}Or_{31}$) to sodic orthoclase ($An_3Ab_{41}Or_{56}$). In the olivine gabbro MM08, plagioclase exhibits a rather large compositional variation from An_{48} to An_{75}. In the monzodiorite MM20, plagioclase is mainly oligoclase (Fig. 7c). Alkali feldspars compositionally cover the range $An_{1–5}Ab_{9–65}Or_{30–90}$. BaO and SrO vary in the range 0.10–0.22 and 0.26–0.74 wt%, respectively. In the foid-bearing diorite MM11 and the theralite MER06, feldspar compositions follow an evolutionary trend from labradorite to oligoclase, anorthoclase and orthoclase (Fig. 7c).

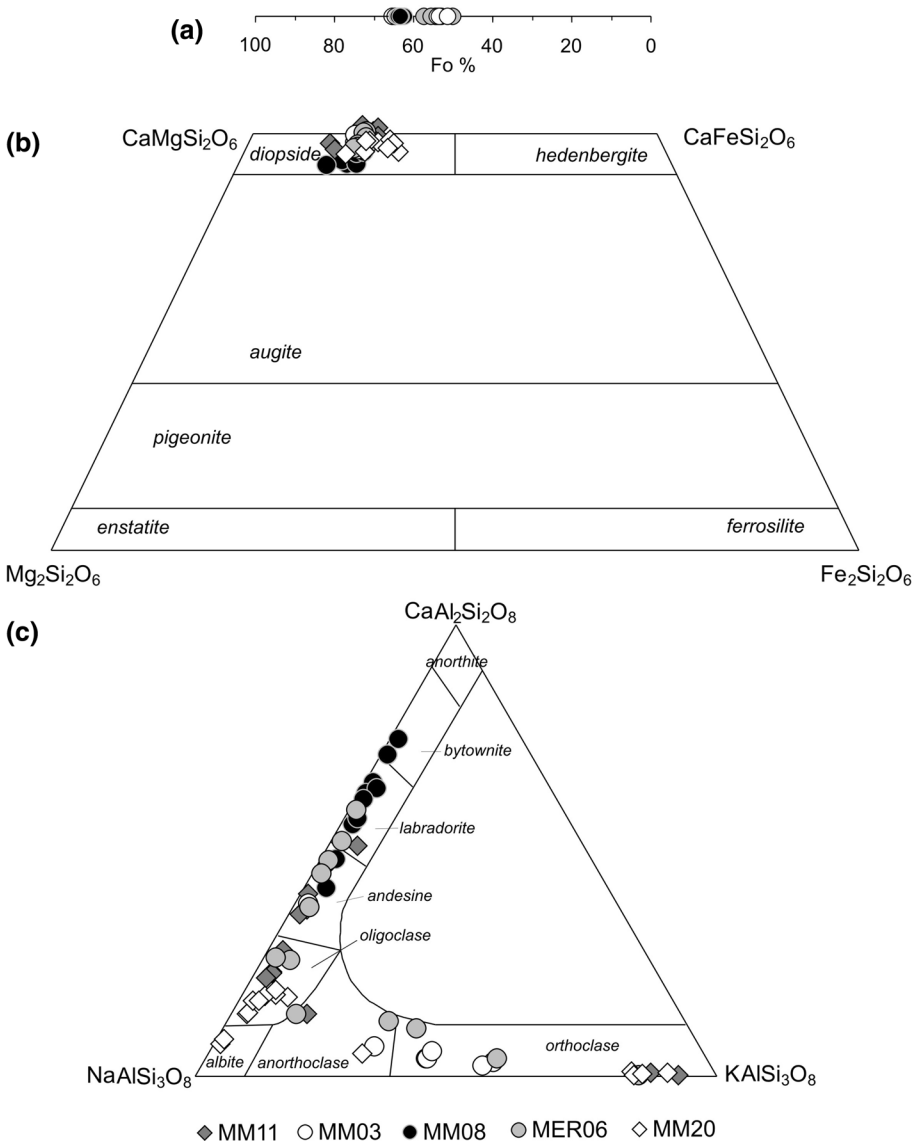

Fig. 7 Mineral compositions in the Mundwara rocks. **a** Olivine. **b** Pyroxenes. **c** Feldspars

Fe–Ti oxides

Magnetite and ilmenite coexist in all samples. Magnetite is the most abundant opaque mineral with a wide compositional range from 1 to 65 mol% ulvöspinel (Fig. 8a). The magnetite with low Ti content occurs in the monzodiorite MM20 and the foid-bearing diorite MM11. MnO is quite variable from 0.07 (monzodiorite MM20) to 1.49 wt% (essexite MM03). Ilmenite contains between 41.75 and 52.74 wt% TiO_2, corresponding to 19–2 % of the haematite end member (Fig. 8a). The MnO concentrations range from 0.96 to 3.81 wt%. Al_2O_3 concentration is always low (<0.5 wt%).

Amphibole

Amphibole occurs in the monzodiorite MM20 and foid-bearing diorite MM11. By the nomenclature of Leake et al. (1997), it is calcic in composition and ranges from pargasite to kaersutite (Fig. 8b). Kaersutite is characterized by high TiO_2 (4.57–5.62 wt%) and moderate MgO (10.23–11.80 wt%) with Mg# ranging from 57 to 64. Pargasite shows similar MgO (9.92–11.20 wt%; Mg# = 53–60) but lower TiO_2 contents (3.95–4.41 wt%). Water contents in amphiboles (Supplementary Table S1-5) have been calculated following Tindle and Webb (1994).

Mica

Mica is present in all Mundwara rocks studied. It has a restricted range of composition in all rock types and plots along the phlogopite–annite tie line (Fig. 8c). Mica crystals have Mg# = 52–72, Al^{IV} = 2.37–2.67 a.p.f.u. (atoms per formula unit) and TiO_2 = 3.03–9.80 wt%. In most cases, the tetrahedral site is not fully filled by Si and Al

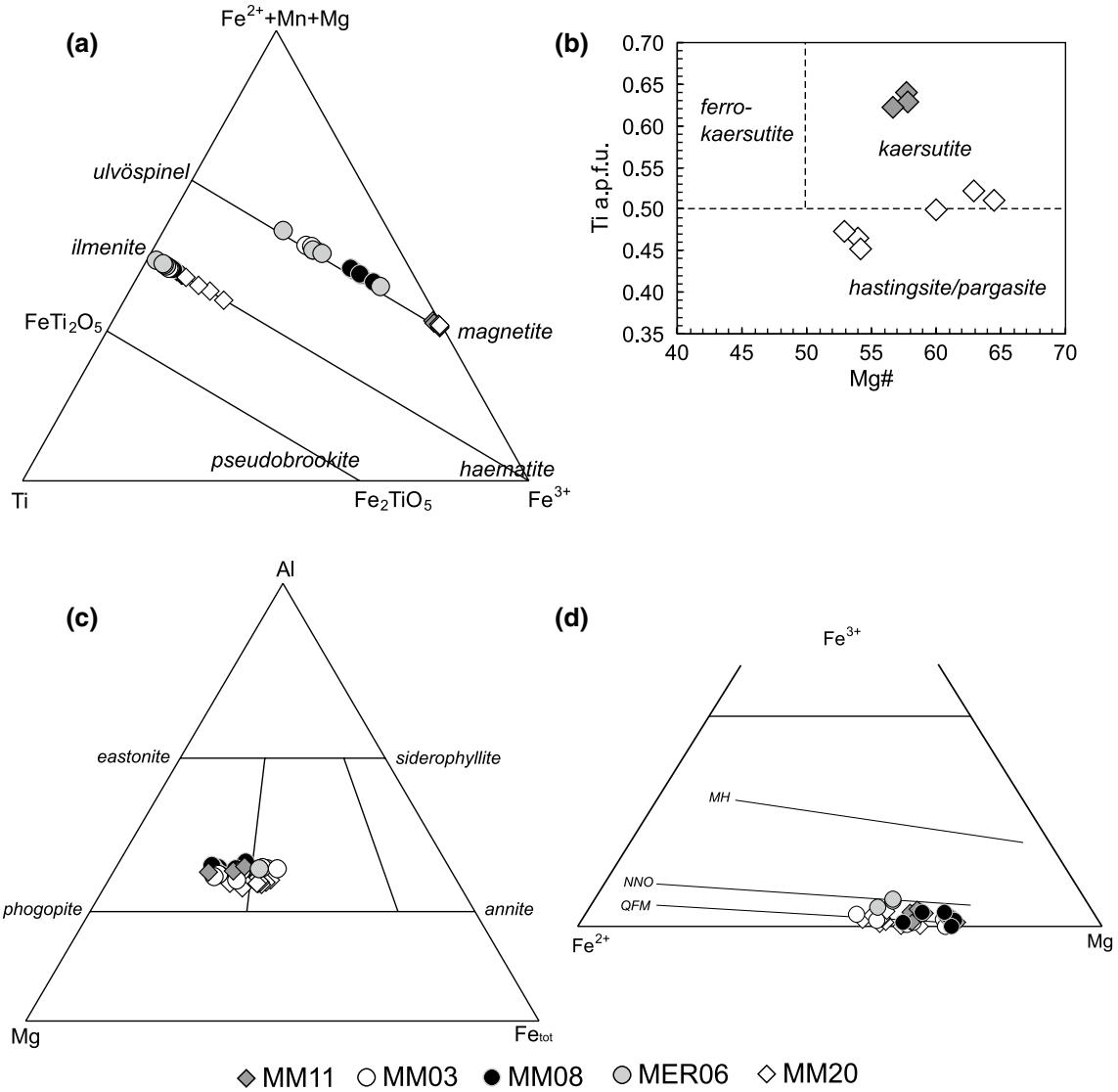

Fig. 8 Mineral compositions in the Mundwara rocks. **a** Fe–Ti oxides. **b** Amphiboles (a.p.f.u: atoms per formula unit). **c** Micas. **d** Fe^{3+}–Fe^{2+}–Mg ternary (Wones and Eugster 1965) diagram for the mica compositions

(Si + Al ranging from 7.72 to 8.00 in calculated structural formulae). It is probably occupied by other cations such as Fe^{3+}.

Feldspathoids

Nepheline occurs as an interstitial phase in the theralite MER06 and essexite MM03. It shows evidence of replacement by analcime in the foid-bearing diorite MM11. Nepheline composition ranges from $Ne_{72}Ks_{16}Qz_{11}$ to $Ne_{80}Ks_{13}Qz_7$ [with molar Na/(Na + K) = 0.83–0.89]. CaO concentrations reach 1.47 wt%.

Accessory phases

Titanite occurs as euhedral crystals in the monzodiorite MM20 and foid-bearing diorite MM11. It has a homogeneous major element composition. ZrO_2 concentration is variable. Apatite typically occurs as inclusions in mica, plagioclase and amphibole. Fluorine ranges from 0.67 to 3.53 wt%. Zircon occurs as tiny grains in the monzodiorite MM20. Zirconolite ($CaZrTi_2O_7$) occurs as small grains in the essexite MM03. Niobium and thorium concentrations range from 7.73 to 9.60 Nb_2O_5 and from 2.79 to 11.05 wt% ThO_2, respectively.

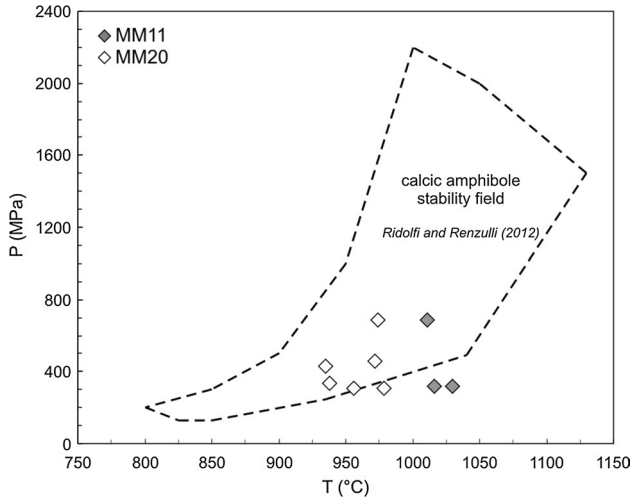

Fig. 9 Pressure–temperature diagram for the Mundwara amphiboles. The calcic amphibole stability field of Ridolfi and Renzulli (2012) is also shown for comparison

Intensive parameters: temperature, pressure and fO_2

The mineralogical data can be used to determine the temperature and pressure conditions of magma emplacement and crystallization. However, it should be noted that these data (derived from mineral assemblages) are strongly dependent on the calibration and, therefore, can provide only provisional geological information.

Pressure estimates were made using clinopyroxene and amphibole geobarometers. The clinopyroxene barometer developed by Nimis and Ulmer (1998) and Nimis (1999) is based on structural parameters. This method is strongly temperature dependent and requires a precise temperature input. Four calibrations are available for pressure calculations. They cover the following compositional ranges: (1) anhydrous basic melts, from basalts through trachybasalts to low-alkali nephelinites (BA), (2) hydrous melts of the same composition (BH), (3) tholeiitic basalts to dacites (TH) and (4) mildly alkaline series from alkali basalt to trachyandesite (MA). Of the four calibrations available, only two (BH and MA) could be applied to our samples. Assuming a mean temperature of 1000 °C, calculated pressures range from 2 to 7 kbar (200–700 MPa). The standard errors estimated by Nimis (1999) for BH and MA calibrations are 2.6 kbar (below 15 kbar) and 2.0 kbar, respectively.

The amphibole thermobarometer of Ridolfi and Renzulli (2012) suggests temperatures of 935–1030 °C and pressure of 686–306 MPa (3–7 kbar) for kaersutite and pargasite crystallization from melts containing 2.8–6.0 wt% H_2O (Fig. 9). Kaersutite is a calcic amphibole stable at high P–T (489–1500 MPa, 960–1130 °C) under relatively oxidizing conditions such as those defined by the NNO buffer with H_2O content in the melt between 3.6 and 5.3 wt% (Ridolfi and Renzulli 2012 and references therein). The temperature and pressure conditions of Mundwara kaersutites are broadly compatible with those obtained by experimental studies (Ridolfi and Renzulli 2012 and references therein). Pressure estimates for calcic amphiboles calculated with the amphibole–plagioclase thermometer of Molina et al. (2015) range from 3 to 6 kbar (300–600 MPa), assuming temperatures between 950 and 1000 °C and plagioclase with labradorite–andesine composition. All estimated pressures indicate that the Mundwara rocks were emplaced and crystallized at middle to upper crustal levels.

The Fe–Ti oxide thermometer and oxybarometer (Spencer and Lindsley 1981) was applied to coexisting ilmenite and magnetite. Calculated temperatures for all magnetite–ilmenite pairs suggest reequilibration during cooling. The highest temperatures are found for the olivine gabbro MM08 (689–788 °C) and the essexite MM03 (742–790 °C). Oxygen fugacities (log fO_2), determined from the model of Spencer and Lindsley (1981), vary between −23.9 and −14.2, and most of the samples are close to the fayalite–magnetite–quartz (FMQ) buffer. However, some samples with lower temperature of equilibration plot above the NNO buffer.

The oxidation states of magma can be also estimated from the mineral chemistry of micas. In the Fe^{2+}–Fe^{3+}–Mg diagram of Wones and Eugster (1965; Fig. 8d), mica compositions for the studied Mundwara rocks fall on the FMQ and NNO oxygen fugacity buffers.

$^{40}Ar/^{39}Ar$ dating

Methods

Eight samples were chosen for dating by the $^{40}Ar/^{39}Ar$ incremental heating technique. These include five biotite separates from mafic rocks (essexite MM03, olivine gabbro MM08, foid diorite MM11, monzodiorite MM20, and tephriphonolite MM24), and three whole-rock nepheline syenites (MM04, MM21 and TOA09). Following Sen et al. (2012), rock chips of about 20–25 g were cut from the hand specimens to avoid veins and weathered material, then crushed and sieved, and biotites in the mafic rocks were picked under the microscope. The 120–180 μm size fraction of the nepheline syenite samples was leached with a 1 % HCl solution to eliminate secondary carbonates, this material and the biotite separates were cleaned in deionised water in an ultrasonic bath, and about 0.02 g of each was packed in aluminium capsules. The Minnesota hornblende reference material (MMhb-1) of age 523.1 ± 2.6 Ma (Renne et al. 1998) and high-purity CaF_2 and K_2SO_4 salts were used as monitor samples. High-purity nickel wires were placed in both sample and monitor capsules to monitor the

neutron fluence variation, which was typically about 5 %. The aluminium capsules were kept in a 0.5-mm-thick cadmium cylinder and irradiated in the heavy-water-moderated DHRUVA reactor at the Bhabha Atomic Research Centre (BARC), Mumbai, for ~100 h. The irradiated samples were repacked in aluminium foil and loaded on the extraction unit of a Thermo Fisher Scientific noble gas preparation system. Argon was extracted in a series of steps up to 1400 °C in an electrically heated ultra-high vacuum furnace. After purification using Ti–Zr getters, the argon released in each step was measured with a Thermo Fisher ARGUS mass spectrometer located at the National Facility for $^{40}Ar/^{39}Ar$ Geothermochronology in the Department of Earth Sciences, IIT Bombay. The mass spectrometer is equipped with five Faraday cups fitted with 10^{11} O resistors.

Interference corrections for Ca- and K-produced Ar isotopes based on analysis of CaF_2 and K_2SO_4 salts were $(^{36}Ar/^{37}Ar)_{Ca}$, $(^{39}Ar/^{37}Ar)_{Ca}$ and $(^{40}Ar/^{39}Ar)_K = 0.000471$, 0.001145 and 0.006842, respectively. ^{40}Ar blank contributions were 1–2 % or less for all temperature steps. The irradiation parameter *J* for each sample was corrected for neutron flux variation using the activity of nickel wires irradiated with each sample. Values of fluence-corrected *J* for various samples are as follows: MM08 Biotite, 0.000537 ± 0.000003; MM11 Biotite, 0.000548 ± 0.000003; MM20 Biotite, 0.000545 ± 0.000003; MM24 Biotite, 0.000540 ± 0.000003; MM04 WR, 0.000527 ± 0.000003; and MM21 WR, 0.000542 ± 0.000003. The plateau ages reported comprise a minimum of 60 % of the total ^{39}Ar released and four or more successive degassing steps. Their mean ages overlap at the 2σ level including the error contribution from the *J* value. The data were plotted using the program ISOPLOT v. 3.75 (Ludwig 2012).

Results

Table 2 gives the summary of the $^{40}Ar/^{39}Ar$ results for six of the eight dated samples which yielded good plateau spectra. Two samples (biotite from the essexite MM03, and the whole-rock nepheline syenite TOA09) did not yield plateau spectra. The stepwise analytical data for the six samples are given in online Supplementary Data Table S2.

The non-plateau argon release spectrum for the MM03 biotites is shown in Fig. 10a and shows an ascending staircase pattern with a prominent step at ~88 Ma comprising 33 % of the total argon release. In comparison, very good plateau spectra are obtained for biotite separates from the olivine gabbro MM08 (82.4 ± 0.4 Ma, Fig. 10b), the foid diorite MM11 (84.6 ± 0.4 Ma, Fig. 10c) and the monzodiorite MM20 (81.3 ± 0.4 Ma, Fig. 10d). Biotite separates from the tephriphonolite MM24 also show a well-developed plateau (80.4 ± 0.4 Ma, Fig. 11a). These four plateau spectra comprise 61–80 % of the total argon release.

Table 2 Summary of $^{40}Ar/^{39}Ar$ dating results for the Mundwara complex

Sample	Plateau					Isochron				Inverse isochron			
	Steps	$\%^{39}Ar$	Age (Ma)	MSWD	*p*	Age (Ma)	Trap	MSWD	*p*	Age (Ma)	Trap	MSWD	*p*
MM08Bio (Ol. gabbro)	8	63.0	82.4 ± 0.4	0.74	0.64	82.2 ± 2.8	299 ± 61	0.10	1.00	82.1 ± 1.5	300 ± 30	0.39	0.89
MM11Bio (Foid dior.)	9	80.1	84.6 ± 0.4	0.15	1.00	84.5 ± 0.7	297 ± 17	0.03	1.00	84.5 ± 0.5	297 ± 10	0.11	1.00
MM20Bio (Monzodior.)	6	68.5	81.3 ± 0.4	0.12	0.99	81.3 ± 1.1	294 ± 22	0.04	1.00	81.3 ± 0.7	295 ± 12	0.09	0.99
MM24Bio (Tephriph.)	8	61.0	80.4 ± 0.4	0.06	1.00	80.5 ± 1.9	295 ± 28	0.01	1.00	80.6 ± 0.8	294 ± 11	0.03	1.00
MM04WR (Ne. syen.)	8	57.5	102.4 ± 0.6	0.12	1.00	102.4 ± 1.4	295 ± 11	0.06	1.00	102.5 ± 1.0	295 ± 7	0.09	1.00
MM21WR (Ne. syen.)	9	70.0	110.4 ± 0.7	0.12	1.00	110.4 ± 1.1	295.6 ± 3.6	0.06	1.00	110.5 ± 0.8	295.4 ± 2.5	0.13	1.00

Trap is initial $^{40}Ar/^{36}Ar$ ratio (trapped component), MSWD is mean square weighted deviate, and *p* is the corresponding probability. Errors are reported at the 2σ confidence level, and monitor mineral is MMHb (523.1 ± 2.6 Ma, Renne et al. 1998). Decay constants used are those of Steiger and Jager (1977). "Bio" indicates biotite separates and "WR" whole-rock sample. GPS locations of the first five samples are given in Table 1, and the location of sample MM21WR is N 24°50.068′ and E 72°32.381′. Two additional samples (MM03Bio, biotite from Musala essexite, and TOA09WR, Toa syenite), were also dated, but did not yield plateau spectra

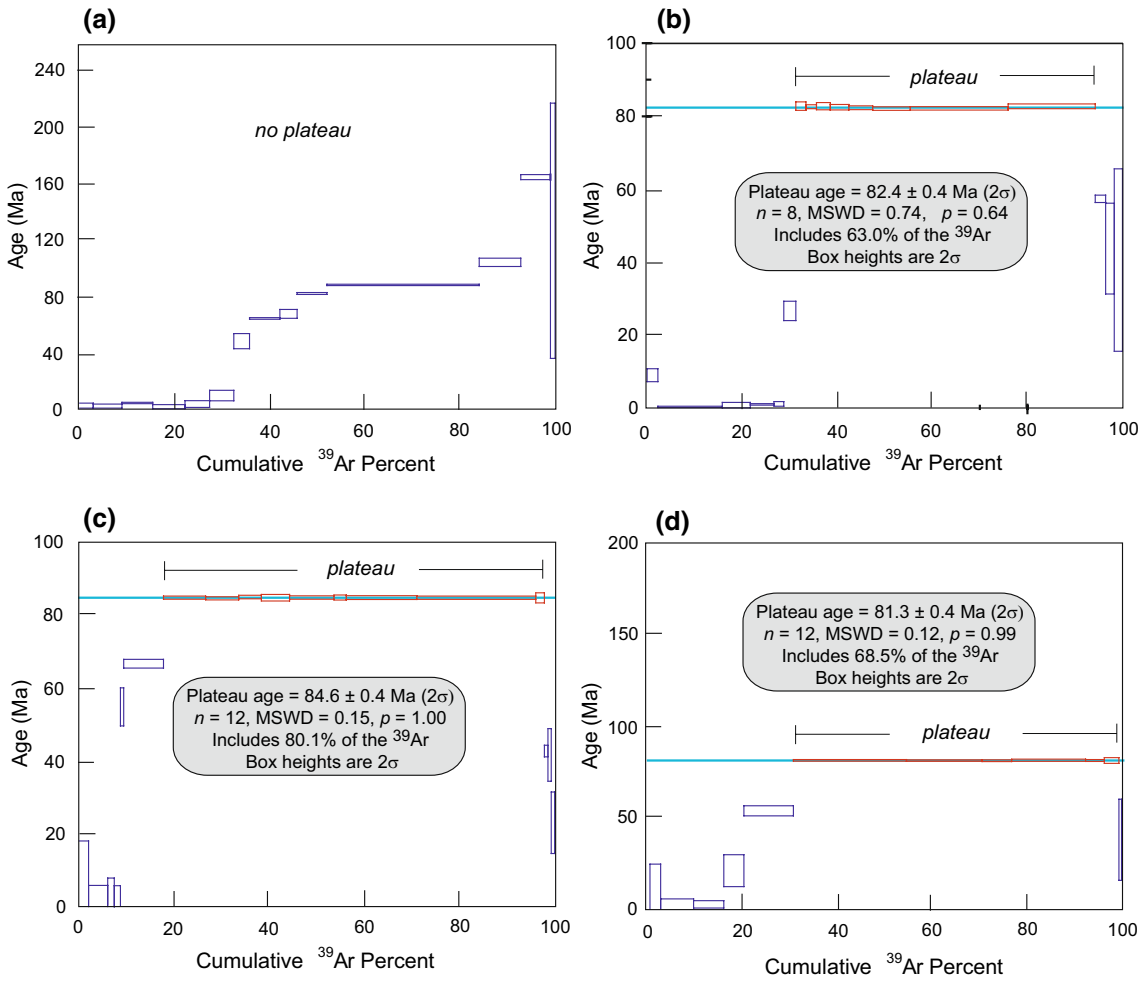

Fig. 10 $^{40}Ar/^{39}Ar$ plateau spectra for the biotite separates from **a** essexite MM03, **b** olivine gabbro MM08, **c** foid diorite MM11 and **d** monzodiorite MM20. The plateau steps are shown with *red outlines* and the non-plateau steps with *dark blue outlines*. Also shown are values of the mean square weighted deviate (*MSWD*) and probability (*p*)

Among nepheline syenite whole rocks, sample TOA09 yielded no plateau but an argon release spectrum with a classic ascending staircase pattern and no prominent age step (Fig. 11b). In contrast, the samples MM04 and MM21 yielded well-developed plateau spectra. MM04 has an age of 102.4 ± 0.6 Ma (57 % argon release, Fig. 11c), and MM21 has an age of 110.4 ± 0.7 Ma (70 % argon release, Fig. 11d).

Discussion

Compositional characters

The studied mafic rocks of Mundwara complex can be divided (on the basis of modal compositions and mineralogical characteristics) into a weakly alkaline gabbro–diorite–monzodiorite suite and a theralite–essexite suite. The mafic rock samples MM03, MM08, MM11, MM20 and MER06 are cumulates with different degrees of alkalinity, comparable to intrusive rocks elsewhere (e.g. Melluso et al. 2005; Cordier et al. 2005).

The olivine gabbro MM08 and theralite MER06 have low Mg# (64–51) and Ni (96–17 ppm) values and Fe-rich olivines ($Fo_{62–65}$ in MM08 and $Fo_{50–58}$ in MER06), which suggest that their parental melts were evolved basaltic liquids. Using MgO-FeO correlation and the composition of the most magnesian olivines, the parental magmas from which such olivines crystallized are estimated to have an Mg# of 30–38. In our calculation, we assumed an olivine-melt Mg–Fe partition coefficient of 0.3 (Roeder and Emslie 1970). Higher Mg# values (41–48) were obtained using the most Mg-rich clinopyroxenes and a pyroxene-melt Fe–Mg partition coefficient of 0.23 (Grove and Bryan 1983). This may indicate that the olivine and clinopyroxene are not in equilibrium. They formed at different stages of crystallization when the Mg# of the liquid was different.

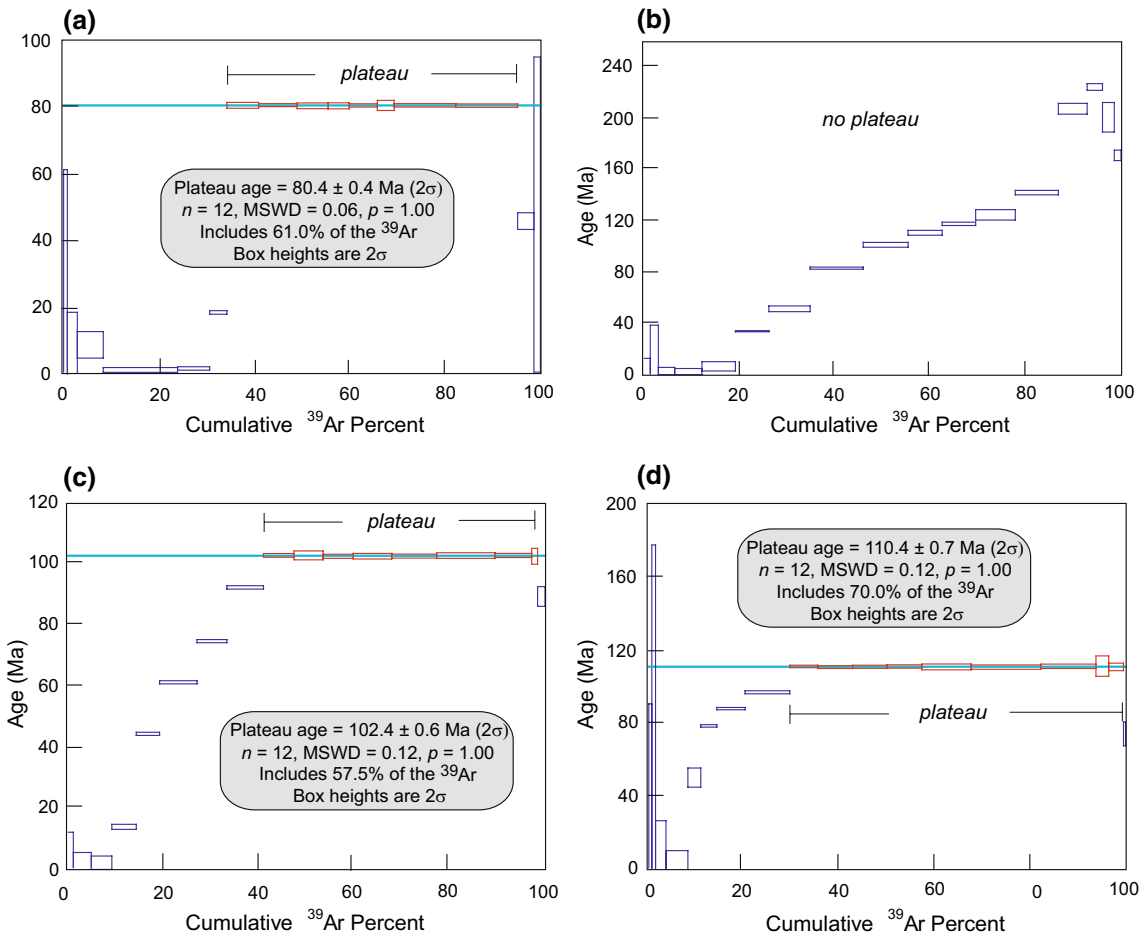

Fig. 11 $^{40}Ar/^{39}Ar$ plateau spectra for **a** biotite separates from tephriphonolite MM24, and whole-rock nepheline syenites **b** TOA09, **c** MM04 and **d** MM21

The presence of kaersutite and nepheline in the Mundwara rocks indicates that the parental melts were of alkaline character. The presence of kaersutite is a feature almost exclusive to mildly alkaline within-plate rocks (Melluso et al. 2005; Cucciniello et al. 2011, 2016; Ridolfi and Renzulli 2012). The parental magmas of the mafic rocks were also sufficiently hydrous for mica and amphibole to form. Kaersutite requires 3.6–5.3 wt% water in the magma (Ridolfi and Renzulli 2012). We discuss a possible source of this water, in a later section.

Existing argon data

Basu et al. (1993) obtained a $^{40}Ar/^{39}Ar$ plateau age of 68.53 ± 0.16 Ma (2σ) on primary biotite from an alkali olivine gabbro in the Toa pluton (relative to a monitor age of 27.84 Ma on Fish Canyon sanidine). They obtained saddle-shaped spectra with minimum step ages of ~71 Ma on amphibole from a ~~metagabbro~~. Saddle-shaped spectra for minerals and whole rocks are considered diagnostic of excess argon (Kaneoka 1974; Lanphere and Dalrymple 1976; Iwata and Kaneoka 2000; Kelley 2002), with the lowest step age as the upper limit to formation time. The amphibole dated by Basu et al. (1993) showed a $^{40}Ar/^{36}Ar$ ratio of 473 ± 5 (much greater than the atmospheric ratio of 295.5) and a 71 Ma maximum possible age. Basu et al. (1993) also dated biotite from an alkali pyroxenite in the Sarnu-Dandali complex in Rajasthan at 68.57 ± 0.08 Ma. They suggested that the Mundwara and Sarnu-Dandali complexes represented Deccan alkaline magmatism that immediately preceded the massive flood basalt phase.

Rathore et al. (1996) dated several compositionally varied samples of the Mundwara suite (essexite, gabbro, basalt, syenites). They obtained $^{40}Ar/^{39}Ar$ ages between 64 and 75 Ma, relative to a monitor age for Minnesota hornblende MMhb-1 of 520.4 ± 1.7 Ma (Samson and Alexander 1987). They obtained saddle-shaped spectra for four of their samples, suggesting a maximum formation age of 71 Ma, and well-developed plateau spectra on two whole-rock syenites from Musala and Mer, with ages of

64.1 ± 0.6 Ma (2σ) and 64.4 ± 0.8 Ma (2σ). They argued that the emplacement of the Mundwara complex was not rapid (as Basu et al. 1993 postulated) but took place over several million years between 71 and 64 Ma.

New argon data

We have obtained several well-developed $^{40}Ar/^{39}Ar$ plateau and isochron ages of 80–84 Ma on Mundwara biotite separates and 102–110 Ma on whole-rock nepheline syenites. These ages are significantly older (up to 40 million years) than those obtained by Basu et al. (1993) and Rathore et al. (1996). Are our $^{40}Ar/^{39}Ar$ ages anomalously high simply due to excess argon, previously identified in Mundwara amphibole (Basu et al. 1993) and Mundwara whole rocks (Rathore et al. 1996)? Excess ^{40}Ar has been recognized in biotites in slowly cooled igneous and metamorphic rocks (e.g. Roddick et al. 1980; Foland 1983) and in biotite and hornblende from the Noril'sk 1 intrusion in the Siberian Traps (Renne 1995). The Neoproterozoic Erinpura Granite that hosts the Mundwara complex could, in principle, have been a major reservoir of excess ^{40}Ar incorporated in the crystallizing Mundwara biotites. Two of our samples, biotite from essexite MM03 (Fig. 10a) and whole-rock nepheline syenite TOA09 (Fig. 11b), both with ascending staircase-shaped argon release patterns, may contain excess argon.

Foland (1983) described case studies in which biotites from slowly cooled rocks yielded well-developed plateau spectra, and yet the plateau ages were anomalously high as identified from regional stratigraphic relationships. More problematic, the evident excess ^{40}Ar could not be identified because even the isochron $^{40}Ar/^{36}Ar$ intercepts had atmospheric values. Foland (1983) cautioned that well-defined $^{40}Ar/^{39}Ar$ plateaus for biotites from metamorphic or slowly cooled rocks cannot be unambiguously interpreted without a priori geochronological or geological information. Such geological or stratigraphic clues to the age of the Mundwara complex are, unfortunately, what is lacking.

However, the broadly similar ages of 68.5–71 Ma obtained by Basu et al. (1993) on both biotite (closure temperature of 300–350 °C, Berger and York 1981; McDougall and Harrison 1999) and hornblende (closure temperature of 550 °C) indicate that the host rocks had cooled relatively rapidly, and therefore, these ages should closely approximate the emplacement age of the intrusions. Similarly, the $^{40}Ar/^{39}Ar$ ages of 80–84 Ma given by biotites in the plutonic rocks MM08 (olivine gabbro), MM11 (foid diorite) and MM20 (monzodiorite), as well as the biotites in the hypabyssal dyke rock MM11 (tephriphonolite), suggest relatively rapid cooling of the complex at this time as well.

Besides, the biotites analysed by Basu et al. (1993) and in this study have well-developed $^{40}Ar/^{39}Ar$ plateaus, and isochrons and inverse isochrons with atmospheric $^{40}Ar/^{36}Ar$ intercepts. Taken at face value, they show no indication of excess argon. What then explains the much higher $^{40}Ar/^{39}Ar$ ages obtained by us compared to those of Basu et al. (1993) and Rathore et al. (1996)? The simplest interpretation of the combined results of these three studies is that all these $^{40}Ar/^{39}Ar$ ages are valid, and the Mundwara complex is polychronous, composed of individual magmatic intrusions emplaced over a long time period from the Early Cretaceous to the Late Cretaceous–Palaeogene. Some of the individual intrusions in the complex are of Deccan Traps age, whereas others are significantly older. This is not unusual. Repetitive magmatism at the same site, sometimes over hundreds of millions of years, is a well-known feature of continental alkaline magmatism (see Barker 1974 for North American examples, and Bailey and Woolley 2005 for African examples).

Geodynamic aspects

The Mundwara complex has usually been considered as a pre-flood basalt alkaline plutonic complex in the Deccan Traps (e.g. Subrahmanyam et al. 1972; Basu et al. 1993; Rathore et al. 1996; Simonetti et al. 1998; Ray et al. 2000). It has been compared to Deccan-age alkaline complexes in the Seychelles (Devey and Stephens 1992; Ganerød et al. 2011). Our new $^{40}Ar/^{39}Ar$ dating results show that the Mundwara complex also represents much older and Deccan-unrelated intrusion events in north-western India, during the Early Cretaceous (~102–110 Ma) and the Late Cretaceous (80–84 Ma). The 102–110 Ma intrusions in the Mundwara complex are thus broadly contemporaneous with the Rajmahal-Sylhet Traps of eastern India (Kent et al. 2002; Ray et al. 2005), whereas the 80–84 Ma Mundwara biotite ages correspond to the late stages of the flood basalt volcanism associated with India–Madagascar breakup (Storey et al. 1995; Pande et al. 2001). Note that no genetic relationships or associations with these provinces are implied.

In Rajasthan itself, a basalt flow has been reported by Bladon et al. (2015) as underlying the Early Cretaceous Sarnu Sandstone in the Sarnu-Dandali area (Fig. 1a). These outcrops occur in the Barmer-Cambay rift which was initiated in the Early Cretaceous due to plate-scale NW–SE-directed extension without a mantle plume (Sharma 2007; Bladon et al. 2015). The basalt in the rift may have formed by higher-degree partial melting of the mantle than the contemporaneous alkaline ultrabasic intrusions at Mundwara outside of the rift. A lamproitic dyke in Kachchh (Fig. 1a) has yielded a U–Pb perovskite age of ~124 Ma (Karmalkar et al. 2014). This indicates that Early Cretaceous alkaline magmatism in north-western India, though not generally recognized, may have been significant.

Geochemical data on the Mundwara complex have typically been interpreted as a guide to the composition of the putative Deccan mantle plume (see Basu et al. 1993; Simonetti et al. 1998). Varied petrological differentiation schemes involving fractional crystallization and liquid immiscibility have been proposed for the derivation of the nepheline syenites and carbonatites of the Mundwara complex from the associated mafic rocks (e.g. Bose and Das Gupta 1973; Chakraborti 1979; Subrahmanyam and Leelanandam 1989, 1991). These are now open to question because of the polychronous nature of the complex with many of its constituent intrusions being genetically unrelated. Also, radiogenic isotopic ratios measured on samples not directly dated and age-corrected to 65 Ma assuming a Deccan Traps association (e.g. Simonetti et al. 1998; Ray et al. 2000) may be significantly undercorrected.

Highly relevant to the question of geodynamics are the primary biotite and amphibole in the Mundwara mafic rocks. These minerals indicate hydrous parental mafic magmas and a hydrated mantle source. Such a source can be a subduction-fluxed, metasomatized mantle wedge which can contain up to 12 wt% water bound in amphibole peridotite (Gaetani and Grove 1998). Hydrous, metasomatized mantle would also melt at relatively low temperatures, thus ruling out an anomalously hot plume. Amphibole is common in the intrusive complexes of the Siberian Traps (e.g. Renne 1995; Ivanov et al. 2008), and a model of active Permian subduction for the Siberian Traps, based on the magmatic water and other arguments, has been offered by Ivanov et al. (2008). Abundant amphibole-gabbro plutons are also known in the Tarim flood basalt province in north-western China and considered to have formed from subduction-related hydrous parental magmas and not a mantle plume (Wan et al. 2013).

There was no active subduction under north-western India during Cretaceous time as it was drifting northwards after separation from Gondwanaland. However, long-lived Jurassic subduction of the Pacific lithosphere occurred under Gondwanaland (Cox 1978), with India a part of it. This subduction, or Precambrian subduction events inferred under north-western India (e.g. Tucker et al. 2001; Dharma Rao et al. 2013), may have hydrated and metasomatized the continental lithospheric mantle beneath Rajasthan. Periodic diffuse lithospheric extension at later times (Early to Late Cretaceous and Palaeogene), resulting in low-degree decompression melting, could have sampled this enriched lithospheric mantle and produced the alkaline magmatism of the Mundwara complex and contiguous areas of Rajasthan and Kachchh.

Conclusions

The Mundwara alkaline plutonic complex in Rajasthan is usually considered a part of the Late Cretaceous to Palaeogene (~65 Ma) Deccan flood basalt province, based on $^{40}Ar/^{39}Ar$ ages of 68.5–64 Ma on biotite, hornblende and whole-rock nepheline syenites (Basu et al. 1993; Rathore et al. 1996). The petrology, mineral chemistry and geothermobarometry of some biotite- and amphibole-bearing mafic Mundwara rocks indicate emplacement of the complex at middle to upper crustal depths. The gabbroic and theralitic rocks are cumulate rocks formed by the accumulation of variable amounts of olivine, clinopyroxene and plagioclase from mildly alkaline parental magmas. Importantly, $^{40}Ar/^{39}Ar$ dating yields plateau and isochron ages of 80–84 Ma on biotite separates from mafic rocks and 102–110 Ma on whole-rock nepheline syenites. There is no evidence for excess ^{40}Ar, and we suggest that these ages, when combined with older ages, indicate that the complex is not simply a Deccan-age intrusive complex but also has significantly older components, i.e. the complex is made of a large number of individual intrusions ranging in age from the Early to the Late Cretaceous and Palaeogene. The Early Cretaceous components broadly correspond in time to the Rajmahal-Sylhet flood basalt province of eastern India, whereas the 80–84 Ma components correspond to the late stages of the Indo-Madagascar flood basalt province. No genetic associations with these provinces are implied, but the Early Cretaceous components in the Mundwara complex and broadly contemporaneous alkaline rocks in Rajasthan and Kachchh may have a common origin in diffuse intraplate lithospheric extension (Sharma 2007; Bladon et al. 2015; Vijayan et al. in press).

The primary biotite and amphibole in Mundwara mafic rocks indicate hydrous parental magmas, derived from hydrated mantle peridotite at relatively low temperatures, thus ruling out a mantle plume source which is anomalously hot by definition. As there was no active subduction beneath north-western India during Early Cretaceous to Palaeogene times, the lithospheric mantle hydration and metasomatism may have occurred during Jurassic subduction under Gondwanaland, or during Precambrian subduction events. Periodic low-degree decompression melting of this hydrated lithospheric mantle from the Early Cretaceous to Palaeogene times, due to diffuse lithospheric extension, produced the Mundwara complex.

Acknowledgments Field work was supported by Grant 09YIA001 to Sheth from the Industrial Research and Consultancy Centre (IRCC), IIT Bombay. We thank Reshma Shinde and Laiq S. Mombasawala for valuable help with the ICPAES analyses at SAIF, IIT Bombay. Funds for EPMA analyses by Cucciniello were provided by Italian MIUR (PRIN Grants 2010–2011 to Leone Melluso). Pande acknowledges Grant No. IR/S4/ESF-04/2003 from the Department of Science and Technology (Govt. of India) towards the development of the IIT Bombay—DST National Facility for $^{40}Ar/^{39}Ar$ Geo-thermochronology. Pande also thanks the IRCC, IIT Bombay, for maintenance support to the Facility (grant 15IRCCCF04). Vijayan was supported by a Ph.D. Scholarship from the University Grants Commission (UGC), Govt. of

India. Jagadeesan thanks Dr. A. Dash, Head, IP and AD, BARC and Dr. S. V. Thakare, IP and AD, BARC, for encouragement and support. Fred Jourdan's detailed review of an earlier version of this paper is greatly appreciated. The present manuscript considerably benefitted from careful journal reviews by Morgan Ganerød and Nilanjan Chatterjee, and the editorial handling of Axel Gerdes.

References

Bailey DK, Woolley AR (2005) Repeated, synchronous magmatism within Africa: timing, magnetic reversals, and global tectonics. In: Foulger GR, Natland JH, Presnall DC, Anderson DL (eds) Plates, plumes and paradigms. Geological Society of America Special Paper 388, pp 365–377

Barker DS (1974) Alkaline rocks of North America. In: Sorensen H (ed) The alkaline rocks. Wiley, London, pp 160–171

Basu AR, Renne PR, DasGupta DK, Teichmann F, Poreda RJ (1993) Early and late alkali igneous pulses and a high-^{3}He plume origin for the Deccan flood basalts. Science 261:902–906

Berger GW, York D (1981) Geothermometry from ^{40}Ar/^{39}Ar dating experiments. Geochim Cosmochim Acta 45:795–812

Bhushan SK, Chandrasekaran V (2002) Geology and geochemistry of the magmatic rocks of the Malani igneous suite and Tertiary alkaline province of western Rajasthan. Geol Surv Ind Mem 126:179

Bladon AJ, Clarke SM, Burley SD (2015) Complex rift geometries resulting from inheritance of pre-existing structures: insights and regional implications from the Barmer Basin rift. J Struct Geol 71:136–154

Bose MK, Das Gupta DK (1973) Petrology of the alkali syenites of the Mundwara magmatic suite, Sirohi, Rajasthan, India. Geol Mag 110:457–466

Chakraborti MK (1979) On the alkali syenites of Mundwara suite, Sirohi district, Rajasthan. Proc Ind Nat Acad Sci 45:284–292

Chakraborti MK, Bose MK (1978) Theralite-melteigite-carbonatite association in Mer ring of Mundwara suite, Sirohi district, Rajasthan. J Geol Soc Ind 19:454–463

Cordier C, Clément J-P, Caroff M, Hémond C, Blais S, Cotten J, Bollinger C, Launeau P, Guille G (2005) Petrogenesis of coarse-grained intrusives from Tahiti Nui and Raiatea (Society Islands, French Polynesia). J Petrol 46:2281–2312

Coulson AL (1933) The geology of Sirohi state, Rajputana. Geol Surv Ind Mem 63:166

Cox KG (1978) Flood basalts, subduction, and the breakup of Gondwanaland. Nature 274:47–49

Cucciniello C, Melluso L, Morra V, Storey M, Rocco I, Franciosi L, Grifa C, Petrone CM, Vincent M (2011) New ^{40}Ar–^{39}Ar ages and petrogenesis of the Massif d' Ambre volcano, northern Madagascar. In: Beccaluva L, Bianchini G, Wilson M (eds) Volcanism and evolution of the African lithosphere. Geological Society of America Special Paper 478, pp 281–282. doi: 10.1130/2011.2478(14)

Cucciniello C, Tucker RD, Jourdan F, Melluso L, Morra V (2016) The age and petrogenesis of alkaline magmatism in the Ampasindava Peninsula and Nosy Be archipelago, northern Madagascar. Mineral Petrol 110:309–331

Devey CW, Stephens WE (1992) Deccan-related magmatism west of the Seychelles-India rift. In: Storey BC, Alabaster T, Pankhurst RJ (eds) Magmatism and the causes of continental break-up. Geological Society, London Special Publications 68, pp 271–291

Dharma Rao CV, Santosh M, Kim SW, Li S (2013) Arc magmatism in the Delhi fold belt: SHRIMP U-Pb zircon ages of granitoids and implications for Neoproterozoic convergent margin tectonics in NW India. J Asian Earth Sci 78:83–99

Eby GN, Kochhar N (1990) Geochemistry and petrogenesis of the Malani igneous suite, north peninsular India. J Geol Soc Ind 36:109–130

Foland KA (1983) ^{40}Ar/^{39}Ar incremental heating plateaus for biotites with excess argon. Isot Geosci 1:3–21

Gaetani GA, Grove TL (1998) The influence of water on melting of mantle peridotite. Contrib Mineral Petrol 131:323–346

Ganerød M, Torsvik TH, van Hinsbergen D, Gaina C, Corfu F, Werner S, Owen-Smith TM, Ashwal LD, Webb SJ, Hendriks BWH (2011) Palaeoposition of the Seychelles microcontinent in relation to the Deccan Traps and the Plume Generation Zone in Late Cretaceous-Early Palaeogene time. In: Van Hinsbergen DJJ, Buiter SJH, Torsvik TH, Gaina C, Webb SJ (eds) The formation and evolution of Africa: a synopsis of 3.8 Ga of Earth history. Geological Society, London Special Publications 357, pp 229–252

Grove TL, Bryan WB (1983) Fractionation of pyroxene-phyric MORB at low pressure: an experimental study. Contrib Mineral Petrol 84:293–309

Ivanov AV, Demonterova EI, Rasskazov SV, Yasnygina TA (2008) Low-Ti melts from the southeastern Siberian Traps large igneous province: evidence for a water-rich mantle source? J Earth Syst Sci 117:1–22

Iwata N, Kaneoka I (2000) On the relationships between the ^{40}Ar–^{39}Ar dating results and the conditions of basaltic samples. Geochem J 34:271–281

Just J, Schulz B, de Wall H, Jourdan F, Pandit MK (2011) Monazite CHIME/EPMA dating of Erinpura granitoid deformation: implications for Neoproterozoic tectono-thermal evolution of NW India. Gondwana Res 19:402–412

Kaneoka I (1974) Investigation of excess argon in ultramafic rocks from the Kola Peninsula by the ^{40}Ar/^{39}Ar method. Earth Planet Sci Lett 22:145–156

Karmalkar NR, Duraiswami RA, Jonnalagadda MK, Griffin WL (2014) Mid-Cretaceous lamproite from the Kutch region, Gujarat, India: genesis and tectonic implications. Gondwana Res 26:942–956

Kelley S (2002) Excess argon in K–Ar and Ar–Ar geochronology. Chem Geol 188:1–22

Kent RW, Pringle MS, Muller RD, Saunders AD, Ghose NC (2002) ^{40}Ar/^{39}Ar geochronology of the Rajmahal basalts, India, and their relationship to the Kerguelen plateau. J Petrol 43:1141–1153

Lanphere MA, Dalrymple GB (1976) Identification of excess ^{40}Ar by the ^{40}Ar/^{39}Ar age spectrum technique. Earth Planet Sci Lett 32:141–148

Leake BE, Woolley AR, Arps CES et al (1997) Nomenclature of amphiboles: report of the Subcommittee on amphiboles of the International Mineralogical Association Commission on new minerals and mineral names. Min Mag 61:295–321

Ludwig KR (2012) Isoplot/Ex, v. 3.75, Berkeley Geochronol Center Special Publication 5

McDougall I, Harrison TM (1999) Geochronology and thermochronology by the ^{40}Ar/^{39}Ar method, 2nd edn. Oxford University Press, Oxford

Melluso L, Morra V, Brotzu P, Tommasini S, Renna MR, Duncan RA, Franciosi L, d'Amelio F (2005) Geochronology and petrogenesis of the Cretaceous Antampombato–Ambatovy complex and associated dyke swarm, Madagascar. J Petrol 46:1963–1996

Middlemost EAK (1989) Iron oxidation ratios, norms and the classification of volcanic rocks. Chem Geol 77:19–26

Molina JF, Moreno JA, Castro A, Rodríguez C, Fershtater GB (2015) Calcic amphibole thermobarometry in metamorphic and igneous rocks: new calibrations based on plagioclase/amphibole Al–Si partitioning and amphibole/liquid Mg partitioning. Lithos 232:286–305

Morimoto N, Fabrie SJ, Ferguson AK, Ginzburg IV, Ross M, Seifert FA, Zussman J, Aoki K, Gottardi G (1988) Nomenclature of pyroxenes. Am Mineral 73:1123–1133

Nimis P (1999) Clinopyroxene geobarometry of magmatic rocks. Part 2. Structural geobarometers for basic to acid, tholeiitic and mildly alkaline magmatic systems. Contrib Mineral Petrol 135:62–74

Nimis P, Ulmer P (1998) Clinopyroxene geobarometry of magmatic rocks, Part 1. An expanded structural geobarometer for anhydrous and hydrous, basic and ultrabasic systems. Contrib Mineral Petrol 133:122–135 (with erratum in 133:314)

Pande K, Sheth HC, Bhutani R (2001) ^{40}Ar–^{39}Ar age of the St. Mary's Islands volcanics, southern India: record of India–Madagascar break-up on the Indian subcontinent. Earth Planet Sci Lett 193:39–46

Pouchou JL, Pichoir F (1988) A simplified version of the "PAP" model for matrix corrections in EPMA. In: Newbury DE (ed) Microbeam analysis. San Francisco Press, San Francisco, pp 315–318

Rathore SS, Venkatesan TR, Srivastava RK (1996) Mundwara alkali igneous complex, Rajasthan, India: chronology and Sr isotope characteristics. J Geol Soc India 48:517–528

Ray JS, Ramesh R, Pande K, Trivedi JR, Shukla PN, Patel PP (2000) Isotope and rare earth element chemistry of carbonatite–alkaline complexes of Deccan volcanic province: implications to magmatic and alteration processes. J Asian Earth Sci 18:177–194

Ray JS, Pattanayak SK, Pande K (2005) Rapid emplacement of the Kerguelen plume-related Sylhet Traps, eastern India: evidence from ^{40}Ar–^{39}Ar geochronology. Geophys Res Lett 32:L10303. doi:10.1029/2005GL022586

Renne PR (1995) Excess ^{40}Ar in biotite and hornblende from the Noril'sk 1 intrusion, Siberia: implications for the age of the Siberian Traps. Earth Planet Sci Lett 131:165–176

Renne PR, Swisher CC, Deino AL, Karner DB, Owens TL, DePaolo DJ (1998) Intercalibration of standards, absolute ages and uncertainties in ^{40}Ar/^{39}Ar dating. Chem Geol 145:117–152

Ridolfi F, Renzulli A (2012) Calcic amphiboles in calc-alkaline and alkaline magmas: thermobarometric and chemometric empirical equations valid up to 1130 °C and 2.2 GPa. Contrib Mineral Petrol 163:877–895

Roddick JC, Cliff RA, Rex DC (1980) The evolution of excess argon in Alpine biotites—a ^{40}Ar/^{39}Ar analysis. Earth Planet Sci Lett 48:185–208

Roeder PL, Emslie RF (1970) Olivine-liquid equilibrium. Contrib Mineral Petrol 29:275–289

Samson SD, Alexander EC Jr (1987) Calibration of the international ^{40}Ar–^{39}Ar dating standard, MMhb-1. Chem Geol 66:27–34

Sen A, Pande K, Hegner E, Sharma KK, Dayal AM, Sheth HC, Mistry H (2012) Deccan volcanism in Rajasthan: ^{40}Ar–^{39}Ar geochronology and geochemistry of the Tavidar volcanic suite. J Asian Earth Sci 59:127–140

Sharma KK (2007) K-T magmatism and basin tectonism in western Rajasthan, India, results from extensional tectonics and not from Réunion plume activity. In: Foulger GR, Jurdy DM (eds) Plates, plumes, and planetary processes. Geological Society of America Special Paper 430, pp 775–784

Simonetti A, Goldstein SL, Schmidberger SS, Viladkar SG (1998) Geochemical and Nd, Sr and Pb isotope data from Deccan alkaline complexes—inferences for mantle sources and plume-lithosphere interaction. J Petrol 39:1847–1864

Spencer JJ, Lindsley DH (1981) A solution model for coexisting iron-titanium oxides. Am Mineral 66:1189–1202

Srivastava RK (1989) Alkaline and peralkaline rocks of Rajasthan. In: Leelanandam C (ed) Alkaline rocks. Geological Society of India Memoir 15, pp 3–24

Steiger RH, Jager E (1977) Subcommission on geochronology: convention on the use of decay constants in geo- and cosmochronology. Earth Planet Sci Lett 36:359–362

Storey M, Mahoney JJ, Saunders AD, Duncan RA, Kelley SP, Coffin MF (1995) Timing of hotspot-related volcanism and the breakup of Madagascar and India. Science 267:852–855

Streckeisen AL (1974) Classification and nomenclature of plutonic rocks. Recommendations of the IUGS subcommission on the systematics of igneous rocks. Geol Rund 63:773–785

Subrahmanyam NP, Leelanandam C (1989) Differentiation due to probable liquid immiscibility in the Musala pluton of the Mundwara alkali igneous complex, Rajasthan, India. In: Leelanandam C (ed) Alkaline rocks. Geological Society of India Memoir 15, pp 25–46

Subrahmanyam NP, Leelanandam C (1991) Geochemistry and petrology of the cumulophyric layered suite of rocks from the Toa pluton of the Mundwara alkali igneous complex, Rajasthan. J Geol Soc India 38:397–411

Subrahmanyam NP, Rao GVU (1977) Petrography, geochemistry and origin of the carbonatite veins of Mer pluton, Mundwara igneous complex, Rajasthan. J Geol Soc India 18:306–322

Subrahmanyam NP, Murali AV, Rao GVU (1972) Age of Mundwara igneous complex—Rajasthan. Current Sci 41:63–64

Tindle AG, Webb PC (1994) Probe-AMPH—a spreadsheet program to classify microprobe-derived amphibole analyses. Comput Geosci 20:1201–1228

Tucker RD, Ashwal LD, Torsvik TH (2001) U-Pb geochronology of Seychelles granitoids: a Neoproterozoic continental arc fragment. Earth Planet Sci Lett 187:27–38

Verma SP, Torres-Alvarado IS, Sotelo-Rodriguez ZT (2002) SINCLAS: standard igneous norm and volcanic rock classification system. Comput Geosci 28:711–715

Vijayan A, Sheth H, Sharma KK (in press) Tectonic significance of dykes in the Sarnu-Dandali alkaline complex, Rajasthan, northwestern Deccan Traps Geosci Front. doi:10.1016/j.gsf.2015.09.004

Viswanathan S (1977) Differentiated dyke rocks of Mer Mundwara, Rajasthan and their metallogenic significance. Geol Mag 144:291–298

Wan B, Xiao W, Windley BF, Yuan C (2013) Permian hornblende gabbros in the Chinese Altai from a subduction-related hydrous parent magma, not from the Tarim mantle plume. Lithosphere 5:290–299

Wones DR, Eugster HP (1965) Stability of biotite: experiment, theory, and application. Am Mineral 50:1228–1272